UNIVERSITÀ DEGLI STUDI DI TRENTO

Dipartimento di Ingegneria Civile Ambientale Meccanica

Corso di Laurea Magistrale in Ingegneria Civile

AFTER-EARTHQUAKE DAMAGE DETECTION: NUMERICAL AND EXPERIMENTAL UNCERTAINTY ANALYSES OF DIFFERENT MONITORING STRATEGIES

Relatore
Prof. Ing. Daniele Zonta

Laureando
Andrea Maroni

Correlatore
Dott. Ing. Davide Trapani

Anno Accademico 2014/2015

Extended Abstract

1 Problem statement

Seismic structural health monitoring systems represent today an important tool for after-earthquake damage assessment of civil structures, allowing for the identification in near real-time of the structures which are safe, or not safe, with regard to possible aftershocks (Çelebi, 2007).

(a) http://spazioinwind.libero.it/sismica/images/managua2.jpg

(b) http://picsant.com/36807548-concrete-column-failure.html

Figure 1: *Typical damages experienced by buildings after a seismic event*

Many structures were unfortunately designed prior to the adoption of seismic design standards. Bringing all the structures up to modern standards is not sustainable for the required costs, and the seismic retrofit of existing buildings is difficult to justify to an owner who has never experienced seismic damage (Çelebi et al., 2004). A building that has been retrofitted is able to resist much greater earthquake forces and has a lower risk of being damaged. Indeed, seismic retrofit of a building does not mean that after the retrofitting the building will never undergo any more damage due to an earthquake. Consequently, damage assessment must be performed for every building involved in a seismic event. In the vulnerability assessment process, the potential damage may be very difficult to quantify and it should be expressed in the form of probability statements only (Porter et al., 2006). A way to quantify numerically the seismic damage sustainable or sustained by a structure is provided by damage indices and the damage evaluation can be based on the results of non-linear dynamic analysis, on the measured response of the structure during the earthquake or on a comparison of modal parameters before and after the earthquake.

The last two methodologies are related to seismic structural health monitoring of structures. In the near future this tool will probably support or even substitute the currently damage assessment methodology, based on visual inspection of structures damaged by the earthquake, mitigating economic losses related to seismic events.

Time is in fact a critical aspect in buildings damage assessment procedure, because buildings cannot attend their regular purpose until they are judged as safe. The speed of evaluation procedure determines the duration for which the potentially damaged buildings remain unusable. The elapsed time directly translates into significant economic losses and to circumstances in which humans are exposed to precarious working and living conditions.

A seismic structural monitoring system is defined in this thesis as a system which allows automated after-earthquake damage classification of a structure by means of a backward analysis. This analysis is based on the collection of a set of observations Y, on the extraction from the set of values of one or more state variables θ representing the state of the structure, and on a model $\mathfrak{M}$, depending on the prior knowledge about the structure, and which links observations to state variable, as can be seen in Figure 2.

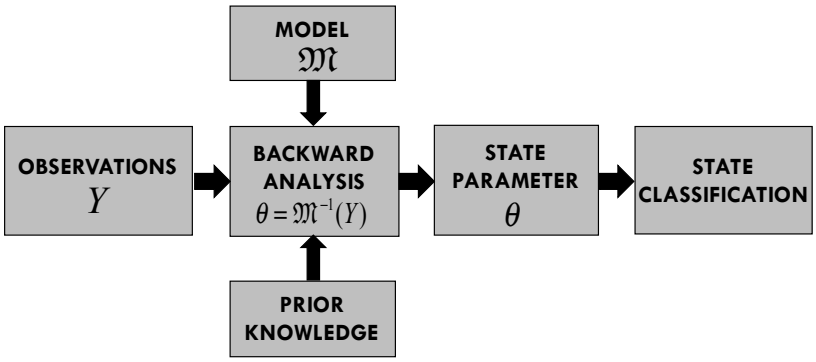

Figure 2: *Logical framework of seismic structural health monitoring*

Purposes of such a system are assessing building usability by aiding the surveyors in damage localization during visual inspection of damaged structures in the emergency phase, by providing the detailed building response data in the following exhaustive damage evaluation phase and by yielding objective information, through the real-time evaluation of the structural response, usable in the decision-making process.

The realization of logical framework depicted in Figure 2 implies the arrangement of a network of sensors in the monitored building for the collection of a set of observations Y of a mechanical quantity q. The data acquisition (DAQ) unit converts the electrical or optical quantity received from sensors into a digital form, which is then used by an artificial intelligence in order to extract one or more features, or state variables, which can be related to structural damage. Raw and processed data can then be transmitted to people involved in the damage assessment process and to a remote database for data storage.

Knowing that, there is a lack in the literature and in international standards of comprehensive guidelines for the design and the management of seismic monitoring systems. The reliability evaluation of monitoring strategies presented in this thesis is performed by following

the instruction reported in the rational framework that can be used in design process of such a monitoring system, developed in (Trapani, 2015). This framework, depicted in Figure 3, relies on the concept of performance-based design, by suggesting a comparison between capacity and demand, in terms of monitoring system accuracy.

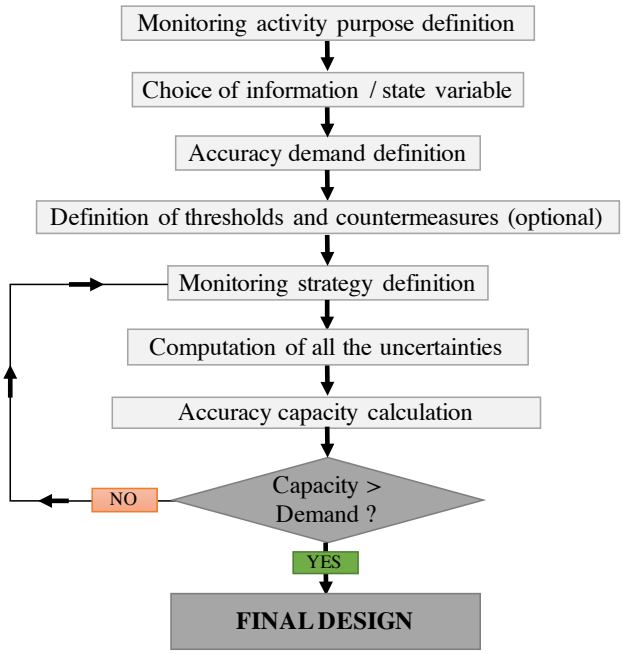

Figure 3: *Flowchart of the design of a monitoring system, adapted from (Trapani, 2015)*

2 Objectives

My aim in this thesis is to study and to define formally the main limitations and uncertainties of after-earthquake damage detection methods of reinforced concrete buildings. Recognizing the inadequacy of currently adopted methodology for after-earthquake damage assessment and a lack of comprehensive guidelines or standards for the design and management of seismic structural health monitoring systems, which then leads to a poor use of them, I have as an objective the reliability evaluation of damage detection strategies performed through seismic monitoring system. Being the precision and the accuracy of system a central aspect of the reported framework for the monitoring system design, I want to investigate formally the accuracy of the currently most used ductility-based method for damage assessment, which is the interstory drift estimation from acceleration measurements alone. In particular I want to study the accuracy dependence on the signal processing techniques performed on data signals before the calculation of displacement and interstory drift ratio, and demonstrate that such a method implies a substantial decrease of accuracy in the estimation of maximum drift in case of inelastic residual displacements at the end of the motion. In closing, I want to study a new propose monitoring method based on acceleration and tilt measurements, developed by *I-kubed* (start up company of the University of Trento), able not only to provide

automatically the residual interstory drift value just after the earthquake, but also to increase the accuracy of the estimation of maximum interstory drift. Therefore, through laboratory tests and numerical analyses performed with MATLAB, I want to precisely evaluate the reliability of this seismic monitoring system in order to solve the problem of damage detection in buildings that sustain inelastic deformation.

3 Summary of the thesis

As said before, in this thesis I dealt with the problem of after-earthquake damage assessment of RC buildings by means of seismic structural health monitoring systems, focusing on the main limitations of currently adopted damage detection methods. I addressed uncertainty analyses of different monitoring strategies, especially those based on response monitoring during the earthquake. Such a family of seismic monitoring systems includes those systems able to monitor in real-time or in quasi real-time the dynamic response of a structure to an earthquake and, in particular, acceleration, displacement and deformation demands. From the displacement-based engineering point of view maximum interstory drift ratio is one of the most influential parameters for the evaluation of seismic performance of existing structural systems. Interstory drift ratio (IDR) is defined as the difference in lateral displacements δ in between two consecutive floors normalized by the interstory height h.

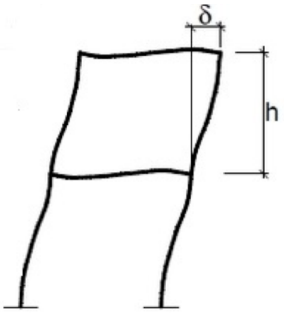

Figure 4: *After-earthquake interstory drift, from (Trapani, 2015)*

3.1 Seismic structural health monitoring

After-earthquake damage assessment is a critical aspect in civil engineering, as it is essential to identify as soon as possible which structures are safe and which are not safe for occupancy, in particular with regard to possible aftershocks. Seismic monitoring systems are capable of automatically detecting structural damage after an earthquake, giving immediate advice about usability and providing quantitative information about structural response to be used in the process of detailed engineering evaluation and retrofitting design. Seismic structural monitoring is a particular branch of structural health monitoring, therefore, the purposes, the state variable, and the monitoring system itself should be chosen and designed as any structural health monitoring system. Consequently, before analysis of the state of the art about seismic SHM systems I started the thesis with the description of a framework for

monitoring system design, justifying that this task would help to understand the motivation of my work. As reported in the title, my thesis addresses uncertainty analyses of different monitoring strategies, therefore the illustration of this capacity-demand way to design a monitoring system (capacity and demand express in terms of accuracy, hence uncertainty) perfectly explains the aim of the following analyses.

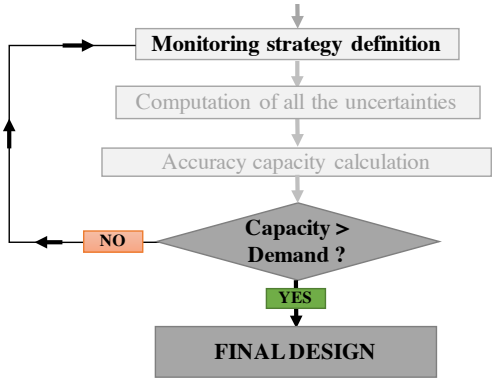

Figure 5: *Comparison between demand and capacity in the flowchart, from (Trapani, 2015)*

Indeed, the performance of a structural health monitoring systems, and therefore of a seismic monitoring system, is evaluated based on the uncertainties of information provided. Consequently, the uncertainty computation is key to assess the reliability of a seismic monitoring system.

Seismic monitoring system must be designed and installed in buildings because current methodology for after-earthquake damage assessment is in-field, visual-based, time consuming, and often subjective. And the duration reduction of damage estimation, possible thanks the automated damage detection of seismic monitoring system, is key to reduce the economic losses. Two of the important methodologies currently used in the world for damage assessment are the procedure provided by Applied Technology Council, based on three placard coloured as a traffic light, and that one based on AeDES manual, published in order to harmonize the post-earthquake safety evaluation of buildings within Europe. After studying how the problem of after-earthquake damage assessment is currently faced, two classes of seismic monitoring systems for damage assessment was described: (i) methods based on changes of modal parameters; (ii) methods in which the damage state of the structure is inferred through the real-time monitoring of the structural response of the structure during the earthquake – namely methods based on ductility demand. Since the use of the former methods still involves several disadvantages, I have focused on the latter methods by describing different methodologies found in the literature. Finally, I reported the displacement-based damage assessment of monitored RC structures, but briefly introducing the damage indices as well. The assessment based on damage indices suffers from epistemic uncertainties that make difficult computing overall uncertainty of the damage index itself. This is mainly due to limited data and knowledge of parameters (epistemicness of the formula). Consequently, seismic monitoring systems based on response monitoring during the earthquake and damage assessment based on displacement and interstory drift are the best monitoring strategies.

3.2 Uncertainty analysis of drift estimation based on acceleration data

As said earlier, I carried out uncertainty analyses of different monitoring strategies because the performance of a structural health monitoring systems is evaluated based on the uncertainties of information provided. Therefore, I discussed the problem of accuracy of seismic monitoring systems based on interstory drift ratio, using only acceleration measurement, because I stated that these monitoring systems and *IDR*-based damage assessment are the best monitoring strategies.

The uncertainties can be divided in two main classes: instrumental uncertainties and model uncertainties. For the former class I have simply reported the instrumental uncertainty analysis carried out in (Trapani, 2015), in order to combine the values found by him with the other source of uncertainty. The instrumental uncertainty was estimate equal to 0.06, considering the possible use of a low-cost sensor as well. In addition to the uncertainties expressed as a percentage, the one caused by instrument noise, which is expressed in units of length, it must also be considered. For displacements less than 10 mm the influence of noise is therefore predominant. This influence, however, decreases increasing the displacement. In other words, when the monitored structure is stiff, or very low thresholds value are desired in the assessment software, a particular attention must be paid in the choice of the accelerometer and to its noise. In the presented analyses the displacement values have never reach quantities less than 10 mm, consequently the instrumental error due to accelerometer noise was neglected.

For the latter class, using the method of double numerical integration of the acceleration measurements alone, I explored the main sources of uncertainties in the estimation of *IDR*. I wanted to know the influence on the overall accuracy of the:

- numerical integration;
- signal process;
- possible residual displacements at the end of the motion.

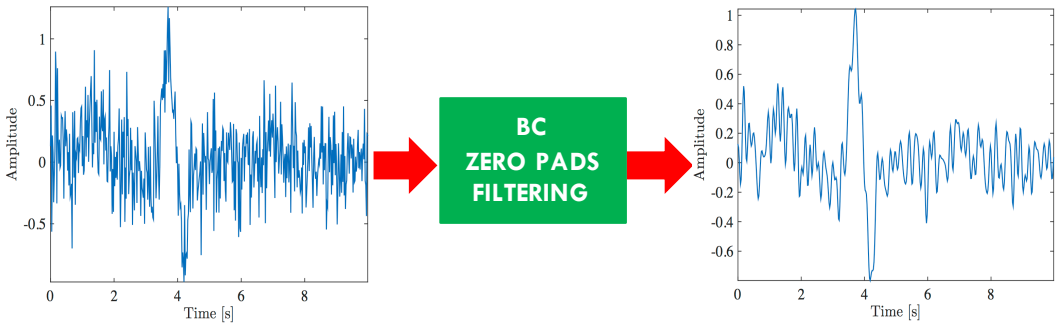

Figure 6: *Example of signal processing of acceleration time-histories (BC means Baseline Correction)*

The uncertainty analysis was carried out by propagating the uncertainties themselves through the procedure of structural drift estimation, described in (Skolnik and Wallace, 2010), which consists of the following steps:

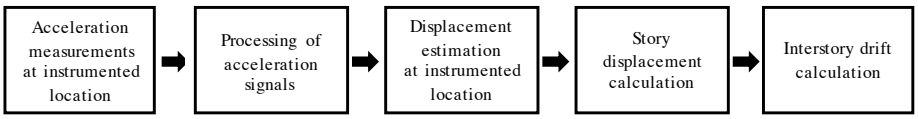

Figure 7: *Steps of the algorithm for interstory drift calculation*

In particular I want to shed some light on how uncertainties propagate through double integration process (performed in the third step of the algorithm depicted above), especially by focusing on their dependence on the low limit of the high-pass filter and on the residual displacement in the estimation of displacements, then employed to calculate the interstory drift.

The parametric analysis was performed on linear and nonlinear SDOF systems.

Error e was computed by comparing the response of the systems obtained from Newmark's integration, assumed as "true", and the "measured" response, obtained by numerically integrating acceleration time-histories.

$$e = \frac{u_{\max} - \hat{u}_{\max}}{u_{\max}} \tag{1}$$

A 4^{th}-order Butterworth high pass filter was implemented to filter acceleration before integration. The cut-off frequency was one of the parameters that were changed to understand the model error variation.

A total of 630 cases were analysed.

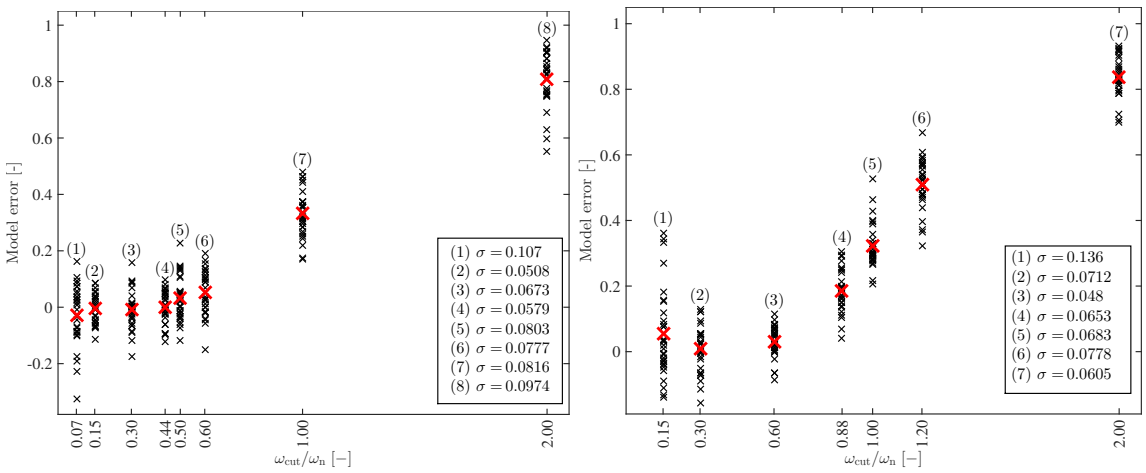

(a) $\omega_{\text{cut}} = 3.77\,\text{rad/s}$ ($f_{\text{cut}} = 0.6\,\text{Hz}$)

(b) $\omega_{\text{cut}} = 7.53\,\text{rad/s}$ ($f_{\text{cut}} = 1.2\,\text{Hz}$)

Figure 8: *Model error variation as a function of the ratio between cut-off and natural frequency*

Figure 8 shows a selection of results of the error by varying the ratio between cut-off frequency and natural frequency. The red crosses represent the mean value of each column, and the legend gives the standard deviation of the error. The other analyses, performed with different values of cut-off frequency, are depicted in Figure 9.

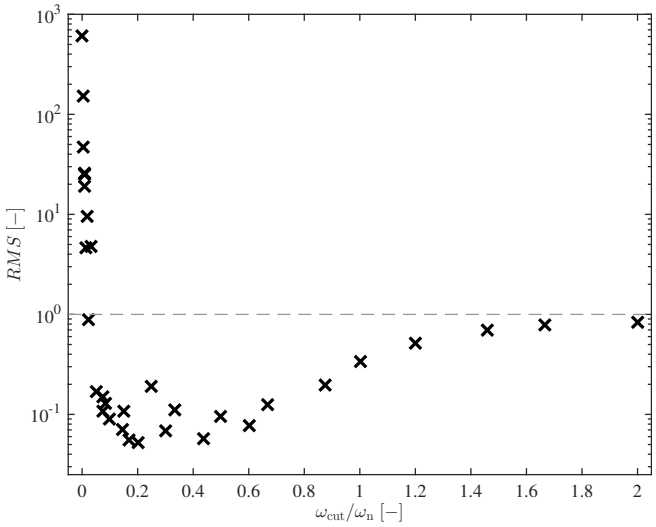

Figure 9: *Error between maximum Newmark displacement and double integration displacement for every ratio of frequencies*

The graphs shows the fluctuation in logarithm scale of the root mean square RMS for the selected ratios of frequencies. The root mean square RMS was computed from the following expression:

$$RMS = \sqrt{\frac{1}{N}\sum_{i=1}^{N} e_i^2} \tag{2}$$

where N is the numbers of model error computed with the same ratio of frequencies.

It can be seen that the trend is composed of two part: a hyperbolic curve for low values of ratio and a second curve that seems similar to the frequency response of the high-pass filter, depicted in Figure 10. The source of uncertainty is different according to the value of the ratio.

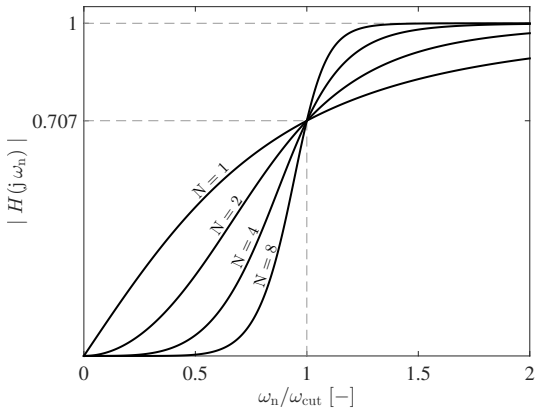

Figure 10: *Frequency response for a Butterworth high-pass filter*

It was confirmed that the error is basically independent on the frequency of the system (all the graphs present the same trend) and that the numerical error is random, characterized by a zero-mean value and a standard deviation of around 0.07. Instead, Figure 9 shows

that the error dependence is strong on the ratio $\omega_{\text{cut}}/\omega_{\text{n}}$ when this one is greater than 0.15. The (mean) error is close to zero when the ratio $\omega_{\text{cut}}/\omega_{\text{n}}$ is lower than or equal to 0.6 and furthermore, as expected, for $\omega_{\text{cut}}/\omega_{\text{n}}$ close to 1 the mean error is around 0.3. This is explained by remembering that the cut-off frequency corresponds to a 0.7 reduction in the component in the signal at that frequency, as can be seen in Figure 10. It is worth emphasizing that only the acceleration was filtered (the velocity was only detrended).

The uncertainty due to the filter is therefore predominant with respect to the numerical error and the error due to noise, and this explains because the trend curve, after a value of the ratio of frequencies approximately equal to 0.15, seems similar to the frequency response of the high-pass filter.

The curve trend when the value of the ratio is less than 0.15 is now studied. Low values of the ratio of frequencies can be obtained from low values of cut-off frequency and the outcomes reported in Figure 9 can be explained by means of the graph in Figure 11.

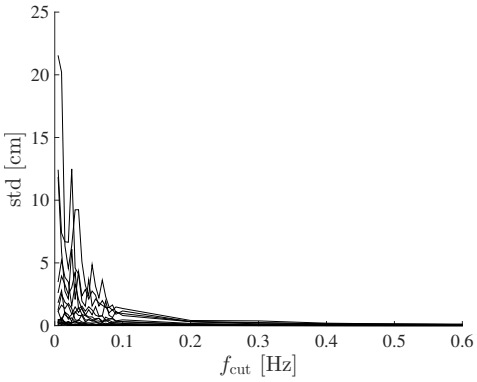

Figure 11: *Uncertainty of double integration displacement due to noise as a function of high-pass frequency cut-off*

This graph reports standard deviation of the displacement obtained by the double integration of noise, modelled such as the sum of Pink and White Noise, for several values of cut-off frequencies. For cut-off frequencies lower than 0.2 Hz the uncertainty due to noise is predominant with respect to the numerical error and to error due to the filter.

The model uncertainty analysis has therefore provided a significant range in which the cut-off frequency must be chosen: it should be chosen between fifteen percent and sixty percent of the frequency of the structure so as to limit the uncertainties due to the presence of the filtering of acceleration, adding that this must still be greater than 0.2 Hz to reduce the uncertainties caused by noise of accelerometer.

The effect of residual displacements at the end of the motion was also investigated. Simple nonlinear analysis of an SDOF was carried out assuming elastic-perfectly plastic force-displacement relation. In these parametric analysis, the ratio between cut-off and natural frequency was chosen as controlling parameter. The behaviour factor q was also chosen as controlling parameter. This factor has allowed to modulate the magnitude of ground acceleration in order to increase the excursion of the structure in its inelastic field.

The table 1 points out all the results obtained from the nonlinear analysis. This table

shows changes in model errors, expressed in terms of RMS, as a function of the selected values of behaviour factor q and of the ratio $\overline{\omega}_c$ between the filter cut-off frequency and the structure's frequency.

Table 1: *Model error, $e^{(I)}$, in the nonlinear case*

		Behaviour factor q [−]					
		1	**2**	**3**	**4**	**6**	**8**
Ratio of frequencies $\overline{\omega}_c$ [−]	**0.01**	34.825	33.296	19.845	27.512	31.720	30.486
	0.1	0.075	0.258	0.360	0.396	0.439	0.457
	0.2	0.067	0.305	0.408	0.457	0.512	0.537
	0.3	0.076	0.327	0.439	0.490	0.551	0.586
	0.4	0.091	0.348	0.470	0.533	0.604	0.636
	0.5	0.110	0.371	0.502	0.571	0.647	0.683
	0.6	0.124	0.400	0.536	0.604	0.680	0.716
	0.7	0.145	0.430	0.573	0.641	0.712	0.746
	0.8	0.186	0.472	0.610	0.676	0.742	0.773
	0.9	0.259	0.521	0.648	0.708	0.770	0.797
	1.0	0.354	0.575	0.688	0.742	0.795	0.818
	1.5	0.736	0.795	0.835	0.855	0.877	0.887
	2.0	0.866	0.884	0.899	0.907	0.917	0.922

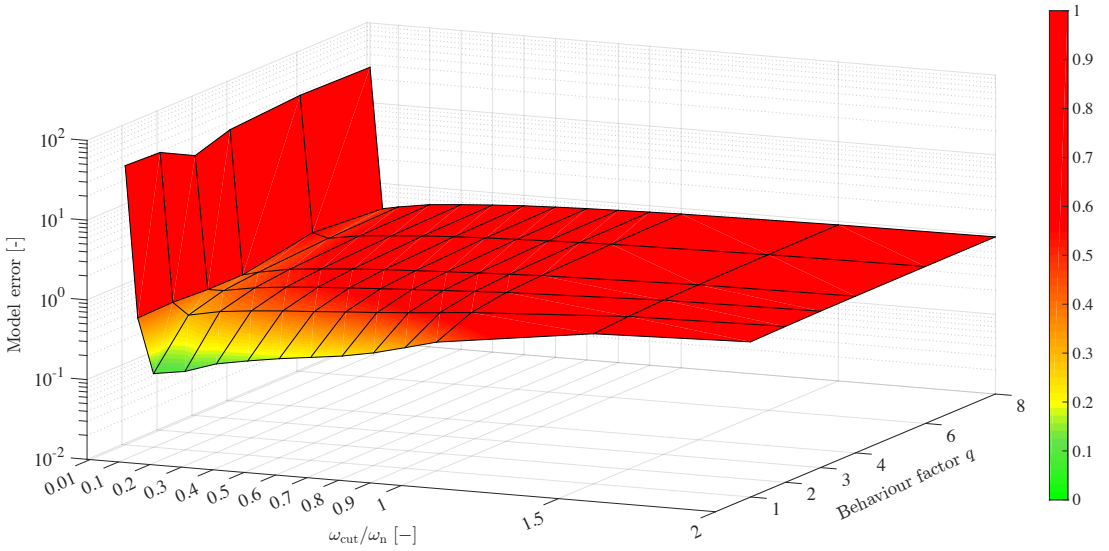

Figure 12: *Variation of model error in the nonlinear analysis, with the behaviour factor, q, and the ratio of frequencies, $\overline{\omega}_c$*

The fluctuation of the model error is also depicted in the three-dimensional graph in Figure 12, where in the two horizontal axes are plotted the two controlling parameters, $\overline{\omega}_c$ and q.

I have therefore found that the method of double integration of acceleration measurements in the case of a nonlinear system suffers from high uncertainties in particular when the

structure sustains high inelastic deformation demands because of the presence of the filter, which cancels the 0 Hz component of the signal. Indeed, in the significant range of the ratio of frequencies, found in the linear analysis, the *RMS* values range between 0.31, when $q = 2$, and 0.72, when $q = 8$, extremely greater than linear results (from 0.07 to 0.12).

The principal source of uncertainty that produce these error increases is, as said earlier, the presence of a residual displacement in the structure. This can be seen in the Figure 13 in which the error, in terms of absolute error between the two models, is related to the residual displacement obtained from Newmark's integration.

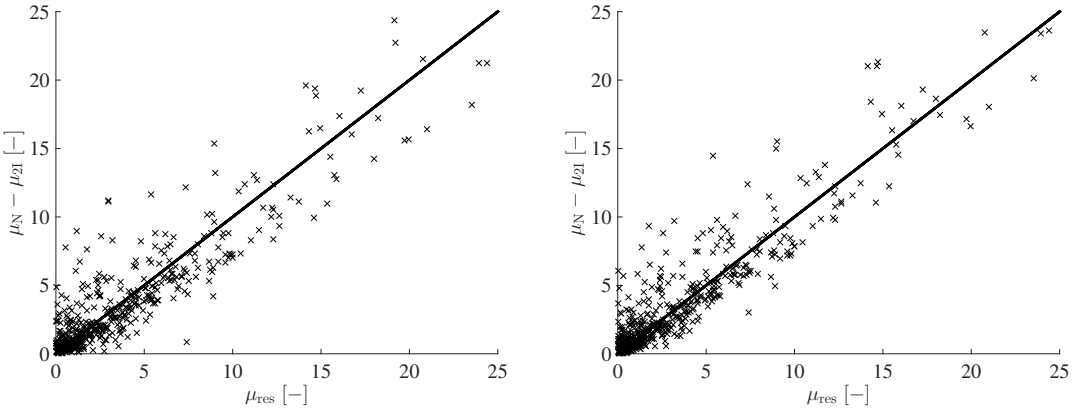

(a) $\overline{\omega}_{\text{cut}} = 0.3$ (b) $\overline{\omega}_{\text{cut}} = 0.4$

Figure 13: *Absolute error $\mu_{\text{N}} - \mu_{2\text{I}}$, with its corresponding residual displacement μ_{res}*

All the quantities reported in the graphs are dimensionless displacements, normalized with respect to the displacement at yielding of the structure, since the analysis was carried out by starting from the equation of motion written in dimensionless form, e.g. in terms of $\mu(t)$ instead of $u(t)$, so that the uncertainty analysis was independent of the yield strength of the system.

A simple approach to solve this problem consists in the addition of residual displacement to the displacement obtained from double numerical method (including band-pass filtering). The permanent displacement is that one obtained with Newmark's integration. This operation leads to a better estimate of the expected value of error but the standard deviation value (and therefore the uncertainty) is slightly decreased (from 0.19 to 0.16) with $q = 2$, but it even increases (from 0.19 to 0.24) for values of q greater than 2, reaching a constant value equal around to 0.24.

The analysis therefore shows that, in the case of structures that exceed their linear limit, the double numerical integration method, using only acceleration measurements, suffers from large uncertainties when it is used for the *IDR* estimation. These uncertainties are due mainly to the choice of the model since the presence of filtering completely erases the permanent displacement. Figure 14 summarises this issue. In the first column are reported the "real" displacement values obtained from Newmark's integration, whereas the second column show the estimation computed with the double numerical integration of acceleration data alone.

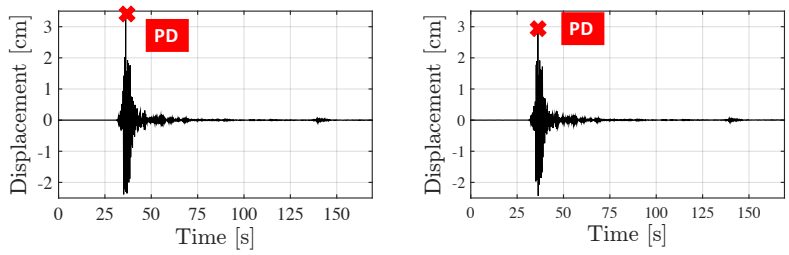

(a) $PD < D_y$

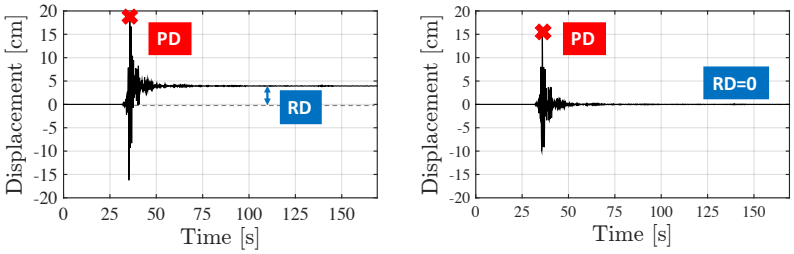

(b) $PD \geq D_y$

Figure 14: *Effect of Residual Displacement (RD) on Peak Displacement (PD) estimation using only acceleration data*

3.3 Drift estimation based on acceleration and tilt data fusion

Recognizing that the interstory drift estimation through double integration using only acceleration measurements in case of nonlinear behaviour of the structure involves large uncertainties due to the presence of a residual displacement, in the following chapter I present a new seismic monitoring system, SAFEQUAKE, developed by *I-kubed* (start up of the University of Trento). It consists of a hinged bar (for example a circular hollow or L steel section) instrumented with 2 bi-axial (or 4 uni-axial) accelerometers measuring accelerations, one (or two) at each end of the beam and remaining parallel to the floors, and one bi-axial inclinometer or accelerometer measuring the tilt of the beam.

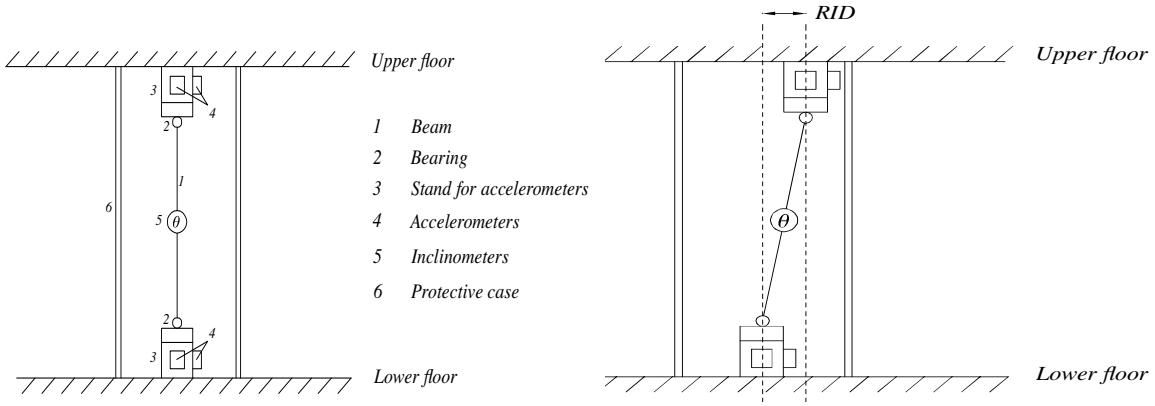

Figure 15: *Schema of the sensing beam, adapted from (Trapani, 2015). Un-deformed configuration on the left, deformed configuration on the right*

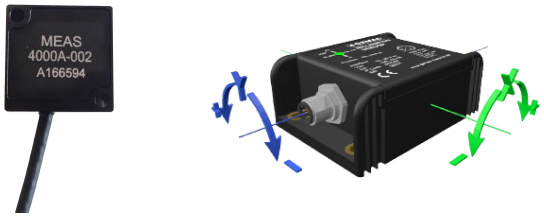

Figure 16: *Uni-axial MEAS 4000A accelerometer and Inclinometer IS2BP090-U-CL*

Accelerometers are fastened to steel cubic supports, in turns rigidly fixed to the floors by means of dowels. The beam is linked to the supports by means of mechanical hinges (e.g., one spherical hinge and one Cardan joint, or two Cardan joints). An inclinometer (or capacitive accelerometer) is fastened to a horizontal plate welded to any point of the beam (e.g., at the mid span). The rigid constraint between supports and floors ensures that accelerometers measure the horizontal accelerations of the floors. During the seismic event, the mechanical hinges ensure that the beam is free to rotate and to tilt of an angle assumed as equal to the ratio of residual differential displacements between the floors and the distance between beam's ends.

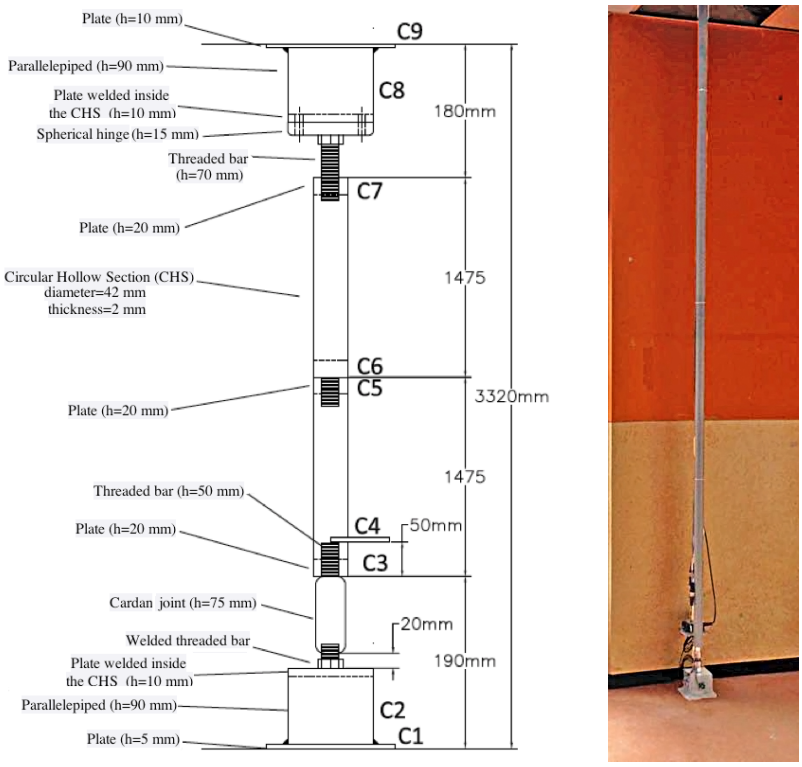

Figure 17: *Detailed schema of sensing beam and an example installed in an elementary school in Trentino, from I-kubed*

The structure of such a monitoring system, the sensing bar and the parallelepiped where it fixed, permits to deploy different monitoring strategies. For instance, the real-time tilt moni-

toring of the bar is possible by means of inclination measurements compensated to the effect of accelerations, without the need of any filtering. Furthermore, a simplified approach, which mitigate the overall uncertainty in the case of a structure that shows nonlinear response, can be performed by adding the residual displacement, measured by the inclinometer, to relative displacement between lower and upper floor obtained from double numerical integration of acceleration measurements (including band-pass filtering). To implement these monitoring strategies different sensor arrangements are possible, such as 2 accelerometers + 1 inclinometer (2A+I) or 3 inclinometers (3I), where 2 inclinometers substitute for the 2 accelerometers at the beam's ends.

The real-time tilt monitoring of sensing bar was firstly studied in a theoretical way, by computing theoretical uncertainties. The equation of motion of the inclinometer tilted by an angle α respect to the direction of gravity is:

$$F = m \cdot g \cos \alpha \tag{3}$$

Instead, the inclinometer subjected to an acceleration $a(t)$ and tilted by an angle θ respect to the direction of gravity can be modelled as a mass m fixed by means of a spring subjected to the inertial force $m \cdot a(t)$ and to the gravity, as depicted in Figure 18.

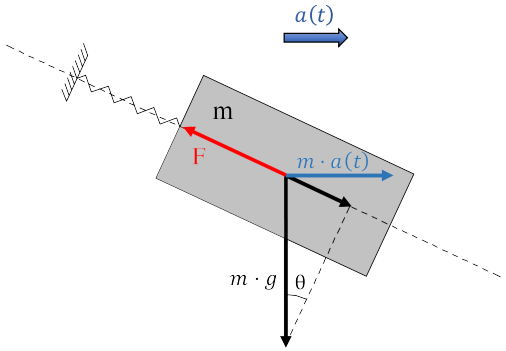

Figure 18: *Forces applied to the inclinometer, adapted from (Trapani, 2015)*

The equation of motion is:

$$F = m \cdot g \cos \theta + m \cdot a(t) \sin \theta \tag{4}$$

The angle was differently named since the inclinometer is subjected to an acceleration that causes in it the measurement of a "fake" angle which is equal to the sum of the angle θ itself and an unrealistic angle due precisely to the acceleration.

$$\alpha_m = \theta + \beta \tag{5}$$

The effect of the dynamically imposed acceleration is that the inclinometer measures a "fake" angle α_m, which includes the effect of imposed acceleration and the actual tilt of the instrument θ (Figure 19).

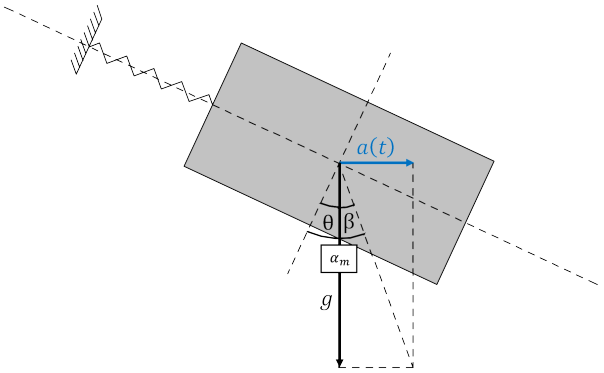

Figure 19: *Effect of imposed acceleration and the actual tilt of the instrument θ*

This latter angle is obtained by solving numerically the equation of motion of the inclinometer written in terms of the unknown angle.

$$m \cdot g \sin\theta + m \cdot a(t) \cos\theta = m \cdot g \sin\alpha_m \tag{6}$$

which leads to:

$$\sin\theta = \sin\alpha_m - \frac{a(t)}{g} \cos\theta \tag{7}$$

This equation can be solved numerically respect to angle θ, knowing the measurement of the inclinometer, $\alpha_m(t)$, and the acceleration to which it is subjected, $a(t)$. The acceleration $a(t)$ can be evaluated by assuming that the field of acceleration is linear between the ends of the bar.

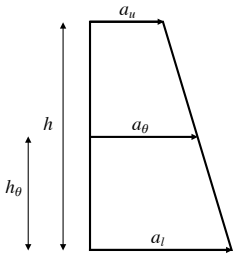

Figure 20: *Linear simplification of the acceleration field*

where a_u and a_l are the accelerations at the upper and lower floor respectively, h is the height between lower and upper floor and h_θ is the height of the inclinometer from the lower floor, as it can be seen in Figure 20. It is therefore clear that the scope of the accelerometers is to estimate the field of acceleration.

The theoretical study of the 3I arrangement differs from the previous one merely for the estimation of the field of acceleration. Indeed, the angle measured by inclinometer is only the "fake" angle because, being fixed to a floor, the sensor is not tilted, then the accelerations at lower and upper floors can be computed as:

$$\begin{cases} a_u = g \tan \alpha_u \\ a_l = g \tan \alpha_l \end{cases} \tag{8}$$

where α_u and α_l are the "fake" angles recorded by inclinometers fixed to the upper and to the lower floor respectively. Finally, the acceleration experienced by the middle inclinometer can be evaluated in the same way described above.

Now that the theoretical operation of the real-time monitoring system has been introduced, I will explain the experimental campaign I conducted in the laboratory. Both sensor arrangements that I calculate the uncertainty were reproduced in the research lab. In particular for (2A+I) arrangement:

- the prototype sensing bar was fixed to the shaking table at its bottom end and at the horizontal part of a steel frame at its other end;
- inclinometer was fixed at about the mid span of the bar;
- one accelerometer was fixed to the shaking table;
- one accelerometer was fixed to the ground, simulating the top floor at rest;
- a laser sensor was used to record the actual displacement of the shaking table.

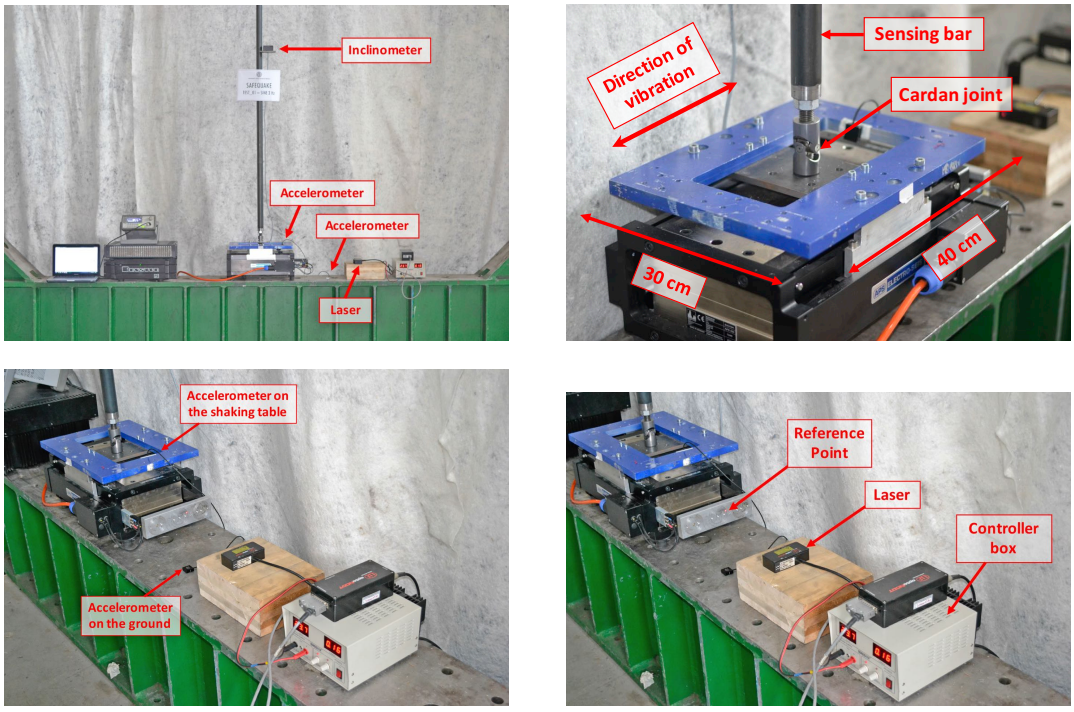

Figure 21: *Sensor arrangement with 2 accelerometers and 1 inclinometers for real-time monitoring of tilt*

While, the 3I arrangement differs from the former only for the presence of two inclinometers instead of the two accelerometers fixed on the shaking table and on the ground.

The shaking table was driven using several displacement time-histories loaded by the operator into the function generator in order to simulate a seismic event, considering both structural linear and nonlinear response. These displacement time-histories was computed from Newmark's integration starting from some of the same acceleration time-histories used in the previous numerical uncertainty analyses. Estimated displacements from acceleration and inclinometer data were compared to a reference laser displacement sensor. Furthermore, the calibration tests for every sensors are carried out in order to obtain the sensitivity of the sensor.

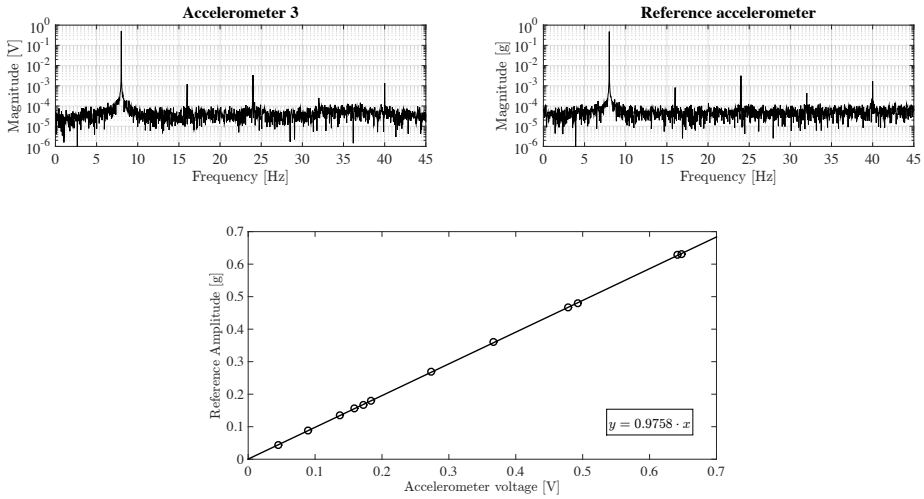

Figure 22: *FFT of the acceleration data and an example of calibration curves of an accelerometer*

The data acquisition procedure is as follow, is the same regardless the used sensor arrangement, and can even be performed by only one operator:

- in the AGILENT 33220A function generator the displacement time-history is selected by operator, setting up its duration in time, say 2 minutes, because the loaded arbitrary wave is continuously run on (as a loop) by the function generator, and setting up the signal peak-to-peak in voltage, say 150 mV;

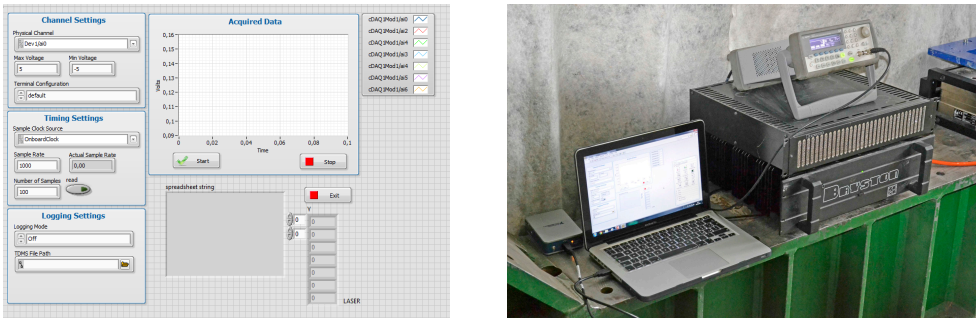

Figure 23: *Acquisition software and AGILENT 33220A function generator*

- the output generator of the AGILENT 33220A and the amplifier are turned on in order to activate the shaking table;

- operator starts the LabVIEW acquisition software, activating the logging mode in order to obtained the text file with all the recorded data;
- the data acquisition and recording of sensors wired starts, by clicking the "Start" button of the application;
- operator stops the acquisition by clicking the "Stop" button, and simultaneously the software asks operator the folder where the text file will be saved;
- once the file with recorded data of all sensors is saved, single test is completed.

Now that I have described the experimental campaign and its procedure, I will report the outcomes obtained from the analyses of data provided by the campaign itself. Some techniques of signal processing were used for improving the quality of the acquired signal, such as subtracting the pre-event mean value or implementing a 8^{th} order Butterworth low-pass filter, before the method for computing the tilt of the sensing bar was performed. A selection of outcomes of the analyses are reported by dividing them in the case of linear response and nonlinear response. The displacement time-histories obtained from calculation written above are graphically compared to the reference time-history acquired from laser sensor. The standard deviation of their difference is computed.

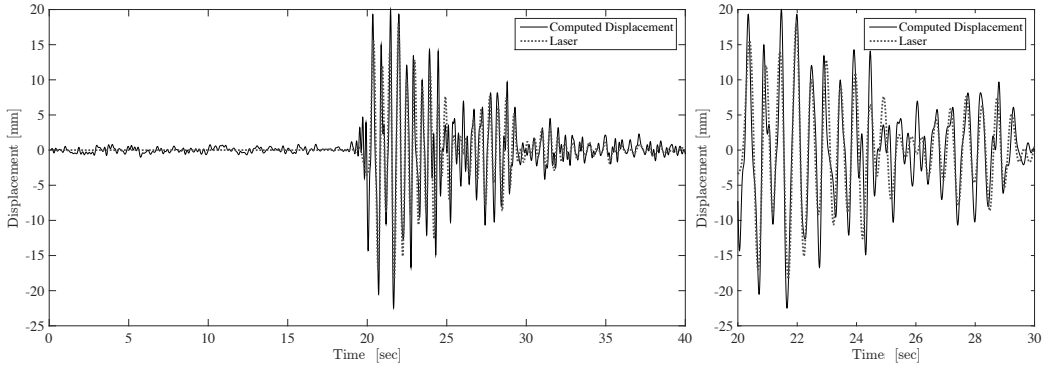

Figure 24: *Computed and laser displacement in the linear case (2A+I)*

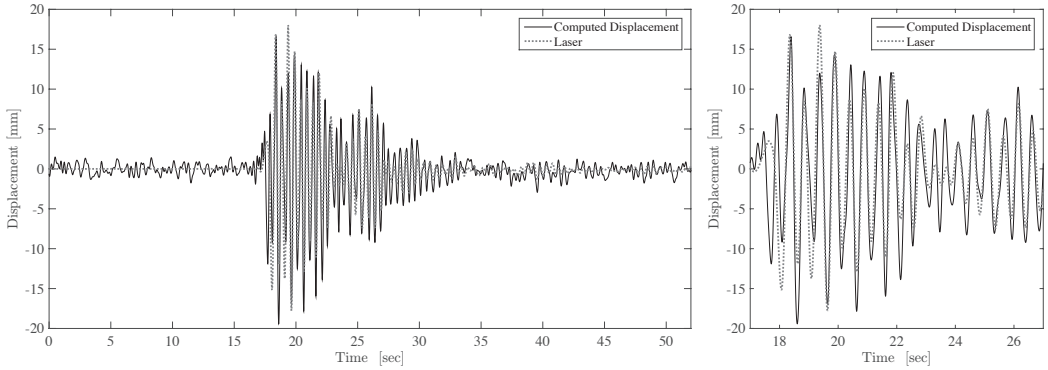

Figure 25: *Computed and laser displacement in the linear case (3I)*

The implemented method for acceleration compensation had as a result that with low-cost sensors it is possible to estimate displacement time-histories during the seismic event with a standard deviation of 2.27 mm for (2A+I) arrangement and of 1.97 mm for (3I) arrangement when the interstory height is 3 m. Instead the accuracy in the estimation of the angle θ (or IDR) is equal to 0.76 mrad and to 0.66 mrad for the two arrangements respectively. The arrangement with three inclinometers provided a greater accuracy than the previous one thanks to the lack of delay between inclinometers. Indeed, the inclinometer is delayed for 0.2 s with respect to the accelerometer.

Using as accuracy demand the limitations on interstory drift ratio for damage assessment defined by Eurocode 8 or other national building standard, the reliability evaluation of this monitoring system, based on a comparison between capacity and demand in terms of accuracy, is completely satisfied.

Similar value of accuracy were also obtained in the case of structural nonlinear response for both sensors arrangements.

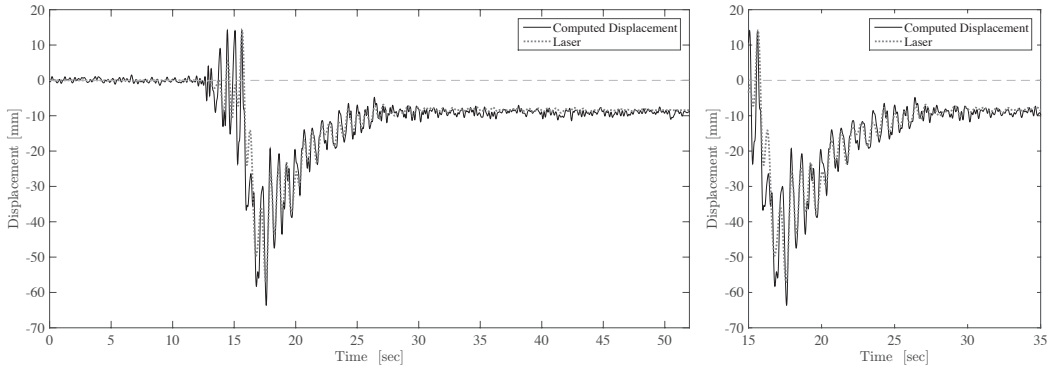

Figure 26: *Computed and laser displacement in the nonlinear case (2A+I)*

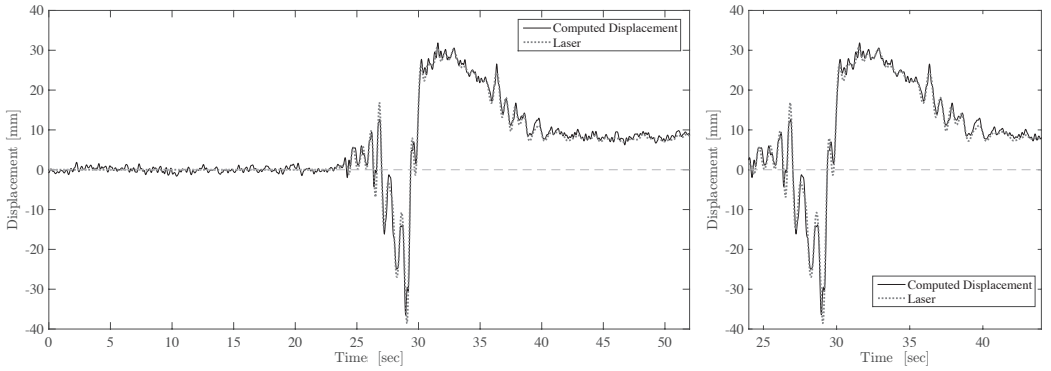

Figure 27: *Computed and laser displacement in the nonlinear case (3I)*

Residual displacement is correctly detected ($\sigma_\delta = 0.67$ mm and $\sigma_\theta = 0.22$ mrad) and no high-pass filters are needed. The performance-based inequality between capacity and demand is satisfied even for the limitations of RID since the accuracy demand is ten times less than the accuracy capacity.

Future Work

I carried out the analyses and the laboratory tests considering that the earthquake experienced by the system is only in one direction. Therefore, the performed analyses do not consider uncertainties in the two main horizontal direction of sensor measurement. A continuation of this work is therefore the analysis of the uncertainty by considering both directions of measurement of monitoring system, since in this thesis the source of uncertainty has been considered considered only in one direction in the analysis of measurement process.

In this thesis I focused mainly on the study of physical parameter provided by monitoring system (e.g. the displacement time-history or the interstory drift ratio) rather than the classification of the state of building. The implementation of the probabilistic approach in the estimation of the state of a seismic monitored structure is therefore the natural continuation of this work. Different structures can suffer different damages because also reaching the same nominal values of the structural parameters their damage will never be the same. Clearly speaking, a monitoring system should provide the probability of a certain level of damage, rather than the level of damage itself. The fragility curves, which basically are the cumulative probability of being in a certain state of structure knowing the demand, should be implemented in the process of damage evaluation.

Finally, the information about the state of a structure provided by seismic monitoring system can be used by decision makers to prepare a pre-earthquake plan, and for the post-earthquake emergency response. Therefore, the development of a real-time (or near-real-time) long-term seismic monitoring system for buildings, which uses Bayesian interpretation of its recorded data and characterized by a decision theory implementation should be studied in the future.

References

Çelebi, M. (2007). Developments in Seismic Monitoring for Risk Reduction. *Journal of Risk Research 10*(5), 715–727.

Çelebi, M., A. Sanli, M. Sinclair, S. Gallant, and D. Radulescu (2004). Real-time seismic monitoring needs of a building owner-and the solution: a cooperative effort. *Earthquake Spectra 20*(2), 333–346.

Porter, K., J. Mitrani-Reiser, and J. L. Beck (2006). Near-real-time loss estimation for instrumented buildings. *The Structural Design of Tall and Special Buildings 15*(1), 3–20.

Skolnik, D. A. and J. W. Wallace (2010). Critical Assessment of Interstory Drift Measurements. *Journal of Structural Engineering 136*(12), 1574–1584.

Trapani, D. (2015). *A monitoring method for after–earthquake damage evaluation of buildings.* Ph. D. thesis, Doctoral School in Engineering of Civil and Mechanical Structural Systems, University of Trento.